Analysis and Design of Speed Control for Torsional Motor Drive Systems

Amin Suyitno[1*] , Dwi Mahadiyan Widya H[2] , Desiana Br Ginting[3]
Fakultas Sains dan Teknologi, Universitas Buddhi Dharma
Jalan Imam Bonjol No. 41, Tangerang, Indonesia
Email: amin.suyitno@buddhidharma.ac.id
Email: *amin.suyitno@buddhidharma.ac.id , desiana.ginting@buddhidharma.ac.id, dwi.mahadiyan@buddhidharma.ac.id

Abstract
This paper presents the analysis and design of speed control for a Torque Motor Drive System. The system presents a torque drive and motor which generally consists of a induction motor and a load connected by a flexible shaft which can be called a Two-Mass Resonance System. To design motor speed controller in this system, a comprehensive and detailed system analysis is required. To realize the design of this control system, it is impossible if the feedback point is taken at the load location, due to the influence of vibration from the flexible shaft. The motor speed control design method used in this paper is to use the Zeroing control design by simulating to see the system output results. From the simulation results, the system output response looks good.

Keyword
Torsional Motor Drive, Flux Vector Control, Disturbance Observer, Zeroing control.

Introduction

Inside the industrial applications like the rolling mill drive systems, the mechanical part of the drive has very low natural resonant frequency because of the large roll inertia and the long shaft in the systems. In some cases, the motor drive systems have more than one roll inertia, but to simplify the analysis, we will discuss the torsional motor drive system as a two-mass-system. To realize the two-mass-systems in this research, the system consists of an induction motor using a flux vector control to represent the motor drive part, and an AC generator which makes it possible to produce various load values for the system. A torsion bar is used as a couple between a motor drive and an AC generator. The different values of the load are possible to obtain if the output AC generator is connected to a variable resistor. In order to obtain high productivity and quick motion in mechanical systems, the mechanism of the torsion bar was designed to minimize the weight on the shaft. Consequently, there are compliances in the mechanical parts especially for train gears and torque transmission mechanisms. The most important compliance here is a mechanical vibration. In this chapter we shall discuss the characteristics of the system and find a model of system in order to get the best method, for the design of the control system. The complete physical system is shown in Figure 1. below.

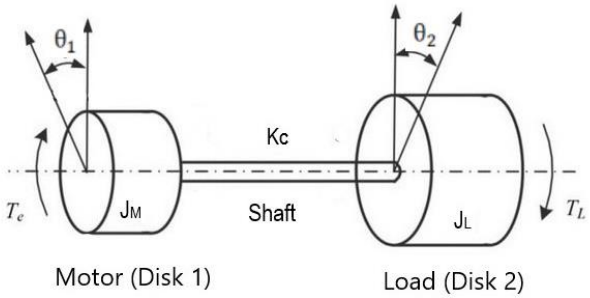

Figure 1. Torsional Motor Drive System

The Analysis of the Mechanical Vibrations

The dynamic behavior of this system can be derived from the equations of motion for each of the disks in Figure 1., where each is taken as a free body. The displacement of disk 1 and disk 2 are θ_1 and θ_2 respectively. When the system in the case is said to be in *equilibrium*, this means that the body as a whole either remains at rest (not rotating at all) or is rotating at a constant rate, and the equations of motion in terms of θ_1 and θ_2 are the following:

$$\begin{aligned} &\text{for disk 1} && J_M\ddot{\theta}_1 + k_C(\theta_1 - \theta_2) = 0 \\ &\text{for disk 2} && J_L\ddot{\theta}_2 + k_C(\theta_2 - \theta_1) = 0 \end{aligned} \quad (1)$$

where J_M and J_L constitute the expressions of motor and generator *moment inertia* and k_C is the *stiffness* of the torsion bar. Since the direction of the torque in disk 1 is opposite to that of disk 2, the torque that works on the end of the torsion bar is certainly opposite to the other, so we can write

$$k_C(\theta_1 - \theta_2) = -k_C(\theta_1 - \theta_2) \quad (2)$$

In the form of Laplace Transform, equation (1) can be written as follows:

$$\frac{\theta_2(s)}{\theta_1(s)} = \frac{J_M s^2 + k_C}{k_C} = \frac{k_C}{J_L s^2 + k_C}$$

Then, by cross-multiplying, we can derive the *characteristic equation*:

$$s^4 + \frac{k_C(J_M + J_L)}{J_M J_L} s^2 = 0$$

Or

$$s^2\left(s^2 + \frac{k_C(J_M+J_L)}{J_M J_L}\right) = 0 \quad (3)$$

It is seen that the characteristic equation of this system is fourth-order in s; but it contains only even powers of s. That is because the system has no damping in it. The result can be obtained as:

$$s = \pm j\sqrt{\frac{k_C(J_M+J_L)}{J_M J_L}} \quad (4)$$

And the *natural frequency* of the system is,

$$\omega = \sqrt{k_C\left(\frac{1}{J_M} + \frac{1}{J_L}\right)} \quad (5)$$

Thus, from this result equation (4) and (5) it is known that the system has one *natural mode of vibration* and *one natural frequency*, some times it is called the *resonance frequency* of two-mass resonant systems. The natural frequency is variable due to load variation and variation of the stiffness of the torsion bar.

Mathematical Model of the Torsional Motor Drive System

A model of the system can be constructed using the same method as in the previous explanation. Where, M represents the *torque* of the motor which is working on the rotor to

produce the torque on the shaft; D_M the *friction factor* of the motor drive; D_L the *friction factor* of the load; D_V the *damping factor* of the torsion bar; and T_L the *disturbance* or *variation of loads* on the system which should be considered. Figure 2. shows a physical model of the system including damping factors and loads.

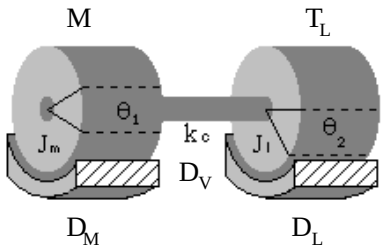

Figure 2. Two-Mass-System with friction

Therefore, the equation of motion in terms of θ_1 and θ_2 are the following:

Disk 1 $\quad M = J_M\ddot{\theta}_1 + D_M\dot{\theta}_1 + k_C(\theta_1 - \theta_2) + D_V(\dot{\theta}_1 - \dot{\theta}_2)$

Disk 2 $\quad 0 = J_L\ddot{\theta}_2 + D_L\dot{\theta}_2 + k_C(\theta_2 - \theta_1) + D_V(\dot{\theta}_2 - \dot{\theta}_1) + T_L$

or in terms of ω_M and ω_L, which represent the motor and load speed, will become:

$$M = J_M\dot{\omega}_M + D_M\omega_M + (\omega_M - \omega_L)\,{}^{k_C}/_{S} + D_V(\omega_M - \omega_L) \quad (6)$$

$$0 = J_L\dot{\omega}_L + D_L\omega_L + (\omega_L - \omega_M)\,{}^{k_C}/_{S} + D_V(\omega_L - \omega_M) + T_L \quad (7)$$

It should be reminded that equations (6) and (7) could be derived because the system is in the equilibrium. Thus the torque in equation (6) is acting in the opposite direction to the torque in equation (7). So, using the same reasoning, the equation below can be derived.

$$(\omega_M - \omega_L)\,{}^{k_C}/_{S} + D_V(\omega_M - \omega_L) = -(\omega_L - \omega_M)\,{}^{k_C}/_{S} - D_V(\omega_L - \omega_M) \quad (8)$$

Just to make the form of the equation simple, $\Delta\boldsymbol{\omega}$ is used to represent the difference of speed; $\Delta\boldsymbol{\omega}=(\omega_M-\omega_L)$. Then rewrite equation (6) in the form of Laplace Transform:

$$\omega_M(s) = \frac{M - \Delta\omega\left({}^{k_C}/_{S} + D_V\right)}{J_M s + D_M} \quad (9)$$

Substituting equation (8) into (7) and reform using Laplace Transform, the angular speed of the second disk can then be written as

$$\omega_L(s) = \frac{\Delta\omega\left({}^{k_C}/_{S} + D_V\right) - T_L}{J_L s + D_L} \quad (10)$$

Since, a flux control method was applied in the motor drive, and the current control loop time constant is small enough to be negligible (1 msec), the value of M(t) equals a constant factor of the inverter k_t, which is multiplied by the motor current $i_a(t)$ [4], shown below

$$M(t) = k_t\, i_a(t) \quad (11)$$

Therefore, by using the combination of equation (10) along with (9), having been substituted by (11), it is possible to draw the complete block diagram of system as shown in Figure (3).

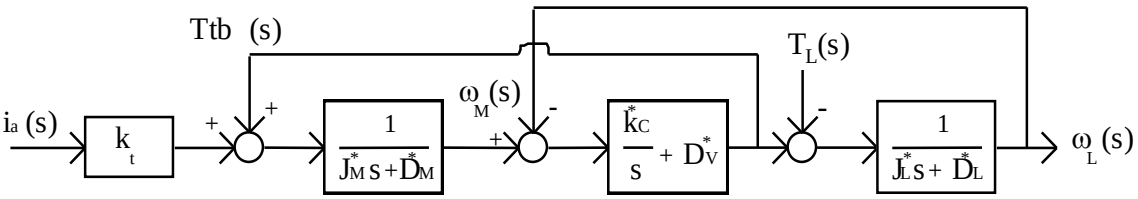

Figure 3. Block diagram of the Two-Mass Resonant System

where, $\Delta\omega = \omega_M(s) - \omega_L(s)$ and $Ttb(s) = \Delta\omega\left({}^{k_C}/_{s} + D_V\right)$, indicates the torque which works on the torsion bar.The following equations represent the output of the system is presented in equation (12); the transfer function of the system without load is presented by equation (13), and the load or disturbance transfer function is equation (14).

$$\omega_L(s) = \frac{(D_V k_t s + k_t k_C) i_a + (J_M s^2 + (D_M + D_V)s + k_C) T_L}{J_M J_L s^3 + (J_M D_L + J_L D_M + D_V J_L + D_V J_M)s^2 + (D_M D_L + J_M k_C + J_L k_C + D_L D_V + D_M D_V)s + D_M k_C + D_L k_C} \tag{12}$$

$$\frac{\omega_L(s)}{i_a(s)} = \frac{D_V k_t s + k_t k_C}{J_M J_L s^3 + (J_M D_L + J_L D_M + D_V J_L + D_V J_M)s^2 + (D_M D_L + J_M k_C + J_L k_C + D_L D_V + D_M D_V)s + D_M k_C + D_L k_C} \tag{13}$$

$$\frac{\omega_L(s)}{T_L(s)} = \frac{J_M s^2 + (D_M + D_V)s + k_C}{J_M J_L s^3 + (J_M D_L + J_L D_M + D_V J_L + D_V J_M)s^2 + (D_M D_L + J_M k_C + J_L k_C + D_L D_V + D_M D_V)s + D_M k_C + D_L k_C} \tag{14}$$

As shown, the transfer function of the plant is a third-order differential equation. It has three poles and one zero, or in the state space formulation we can derive:

$$\dot{\mathbf{X}} = \mathbf{A}\mathbf{X} + \mathbf{B}u + \mathbf{D}T_L \tag{15}$$

$$y = \mathbf{C}\mathbf{X}$$

$$\mathbf{X} = \begin{bmatrix} \theta_M \\ \omega_M \\ \theta_L \\ \omega_L \end{bmatrix}; \quad \mathbf{A} = \begin{bmatrix} 0 & 1 & 0 & 0 \\ -\frac{k_C}{J_M} & -\frac{D_M + D_V}{J_M} & \frac{k_C}{J_M} & \frac{D_V}{J_M} \\ 0 & 0 & 0 & 1 \\ \frac{k_C}{J_L} & \frac{D_V}{J_L} & -\frac{k_C}{J_L} & -\frac{D_V + D_L}{J_L} \end{bmatrix}; \quad \mathbf{B} = \begin{bmatrix} 0 \\ \frac{k_t}{J_M} \\ 0 \\ 0 \end{bmatrix}; \quad \mathbf{C} = \begin{bmatrix} 0 \\ 1 \\ 0 \\ 0 \end{bmatrix}; \quad \mathbf{D} = \begin{bmatrix} 0 \\ 0 \\ 0 \\ -\frac{1}{J_L} \end{bmatrix}$$

Most of the control analysis neglects the damping factors, without effecting the accuracy of analysis because the former are too small. So, the transfer function from input T_r to ω_L can be written as follows,

$$\frac{\omega_L(s)}{i_a(s)} = \frac{k_t k_C}{J_M J_L s^3 + (J_M k_C + J_L k_C)s} \tag{16}$$

and its characteristic of the frequency response is shown in Figure 4. It shows that the system is internally unstable. Its resonance frequency can be obtained from equation (5). To design the controller of this system, in some cases, the transfer function in different form are needed, which takes the output of the motor drive as the output of the system. The transfer function is easy to obtain as shown in equation (17) and the characteristic of the frequency response is described in Figure 5.

$$\frac{\omega_M(s)}{i_a(s)} = \frac{k_t(J_L s^2 + k_c)}{J_M J_L s^3 + (J_M k_C + J_L k_C)s} \tag{17}$$

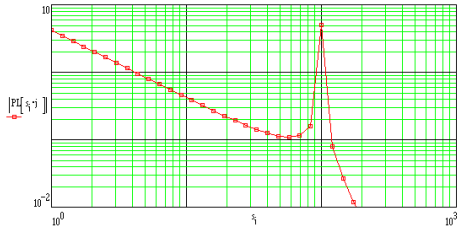

Figure 4. The frequency response of $\frac{\omega_L(j\omega)}{i_a(j\omega)}$;

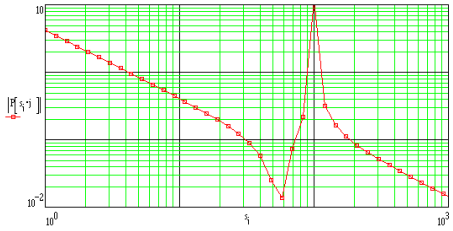

Figure 5. The frequency response of $\frac{\omega_M(j\omega)}{i_a(j\omega)}$.

Speed Control Design by Zeroing Method for this Flexible System

As mentioned before, this system is rather special, it is unstable inside in the system. The control design has to cover not only the robustness of the parameter's variations, but it also has to have a capability to reduce the flexibility of the shaft, moreover when a disturbance acts on the system. The control method that was applied in this system is a zeroing technique with an equivalent disturbance observer. The method's approach used a design which enables the plant, to be seen part by part. Referring to our plant, which is to be controlled in Figure 3, it was explained that the plant is a combination of the motor drive and the load. It was noticed that the combination was from equation (9) for the motor drive, and equation (10) for the loads, so we can rewrite those equations as

$$J_M s\omega_M + D_M\omega_M + Ttb(s) = k_t i_a(s) \tag{18}$$

and

$$J_L s\omega_L + D_L\omega_L + T_L(s) = Ttb(s) \tag{19}$$

respectively, since $Ttb(s) = \Delta\omega\left(\frac{K_C}{s} + D_V\right)$, where $\Delta\omega$ is the difference of motor speed and load speed. Between those parts there are feedback connections, Ttb and ω_L. One is connected to the place between the inverter and the induction motor, and the other one to the output of induction motor. Whenever, the disturbances act at the input T_L, the feedback Ttb has a greater influence on the system than the other, because it goes to the input of the motor drive. Therefore, in order to eliminate the disturbances in the plant, the overall system should have two (2) equivalent disturbance observers, one covering the disturbance T_L , in the load part, and the other one covering Ttb in the motor drive part. In the following description there are called 1. Flexible Cancellation (*FCAN*) and 2. Motor Cancellation (*MCAN*) which are discussed in the next section. In addition to these controllers, in order to achieve a quick command response for the system, a feed-forward controller is also be added.

The Control Design

It is understood that the exact value of the physical parameters of the plant may be different from the nominal values which are written in the specification from factories. The effect of nonlinearities and disturbances also has to be considered, so

$J_M = J_M^* + \Delta J_M$; $D_M = D_M^* + \Delta D_M$; $J_L = J_L^* + \Delta J_L$; $D_L = D_L^* + \Delta D_L$
$k_t = k_t^* + \Delta k_t$; $k_c = k_c^* + \Delta k_c$; $k_c = k_c^* + \Delta k_c$; $D_V = D_V^* + \Delta D_V$

where * denotes the nominal value of the parameters and Δ represents the deviation values or unknown values.

1. Motor Cancelation (MCAN) and the Feed-Forward Controller Design

First, the nominal and the deviation values were substituted as described above in equation (18), so that the equivalent system and the equivalent Ttb(s), $Ttb_e(s)$ are defined as

$$Ttb_e(s) = \Delta J_M s\omega_M(s) + \Delta D_M \omega_M(s) - \Delta k_t i_a(s) + Ttb(s) \tag{20}$$

The physical meaning of the symbols written in the first term up to the fourth on the right hand side of the equation (20) is the torque due to parameter variation, the variation of viscous frictions torque, the torque variation due to the flux vector control failure and torque ripples, and external load torque or external disturbance passed through the feedback respectively. Except form equation (20), through an equivalent system, which using the nominal values, as well as Ttb_e, the following equation can be derived.

$$Ttb_e(s) = k_t^* i_a(s) - J_M^* s\omega_M(s) - D_M^* \omega_M(s) \tag{21}$$

To obtain the estimate $Ttb_e^*(s)$ of $Ttb_e(s)$, the following observer is constructed by using a low pass filter $\frac{1}{(T_0 s+1)}$, so $Ttb_e^*(s)$ is

$$\mathrm{Ttb}_e^*(s) = \frac{\mathrm{k}_t^* \mathrm{i}_a(s) - (\mathrm{J}_M^* s + \mathrm{D}_M^*)\omega_M(s)}{\mathrm{T}_0 s + 1} \tag{22}$$

where T_0 is the time constant of the observer, and the change of signal Ttb_e is assumed to be slow so that the observer can follow. Next, in order to cancel the Ttb_e, the estimate signal, Ttb_e^* is multiplied by the inverse of k_t^* and is then added to the input i_a^* as shown in Figure 6, below.

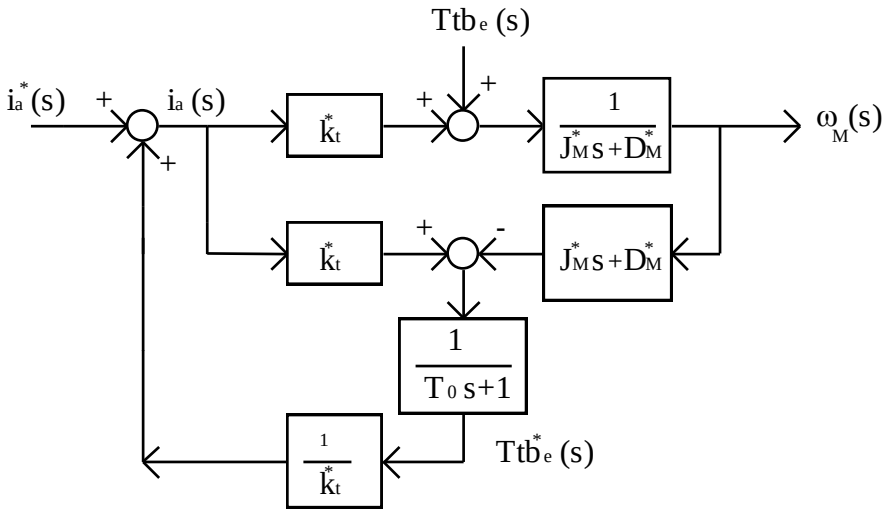

Figure 6. Block diagram of motor drive and equivalent disturbance observer

Hence, it is easy to understand that using the equivalent disturbance observer as shown in the Figure 6, the signal Ttb_e can be canceled as explained below. Calculate the overall differential equation which is in s form of the system which shown in motor site, assuming i_a^* equals zero or the system is in the steady state condition.

$$\omega_M(s) = \frac{\left.(1+T_0 s)\right/\{T_0 s(J_M^* s+D_M^*)\}i_a - \left.Ttb_e\right/(J_M^* s+D_M^*)}{1+\left\{\left.(1+T_0 s)\right/T_0 s(J_M^* s+D_M^*)\right\}\left\{\left.(J_M^* s+D_M^*)\right/(1+T_0 s)\right\}} \tag{23}$$

Then, the equivalent block diagram of Figure 6 can be shown as,

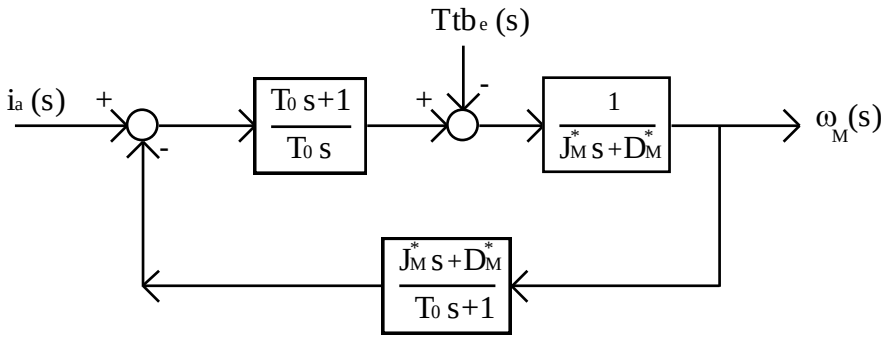

Figure 7. Equivalent block diagram of Figure 3.1.

It is shown that a PI controller is contained in this controller. To see the influences of signal Ttb_e in the closed-loop system, first defines the transfer function $\omega_M(s)/Ttb_e(s)$ from equation (23), as shown in equation (24) below.

$$\frac{\omega_M(s)}{Ttb_e(s)} = \frac{-1}{\left(1+\frac{1}{T_0}s\right)\left(J_M^* s+D_M^*\right)} \tag{24}$$

Since the time constant of the filter, T_0 is very small, $\frac{\omega_s(s)}{Ttb_e(s)}$ becomes zero quickly. Hence, this method is called *zeroing* [1]. The eigenvalues of the system are discussed in later. In the controller of the motor drive part, in addition to MCAN, the system consisted of a feed-forward controller in order to achieve a quick command response in the systems. For that purpose, the feed-forward controller can be obtained using inversion of the motor drive system (the motor drive plus the constant factor of the inverter) and additional k_p as a gain of the proportional controller of the system. It follows from [1], that the value of k_p can be determined from

$$\frac{J_M^*}{k_t^* k_p} >> T_0 \tag{25}$$

Therefore, Figure 3.4 becomes

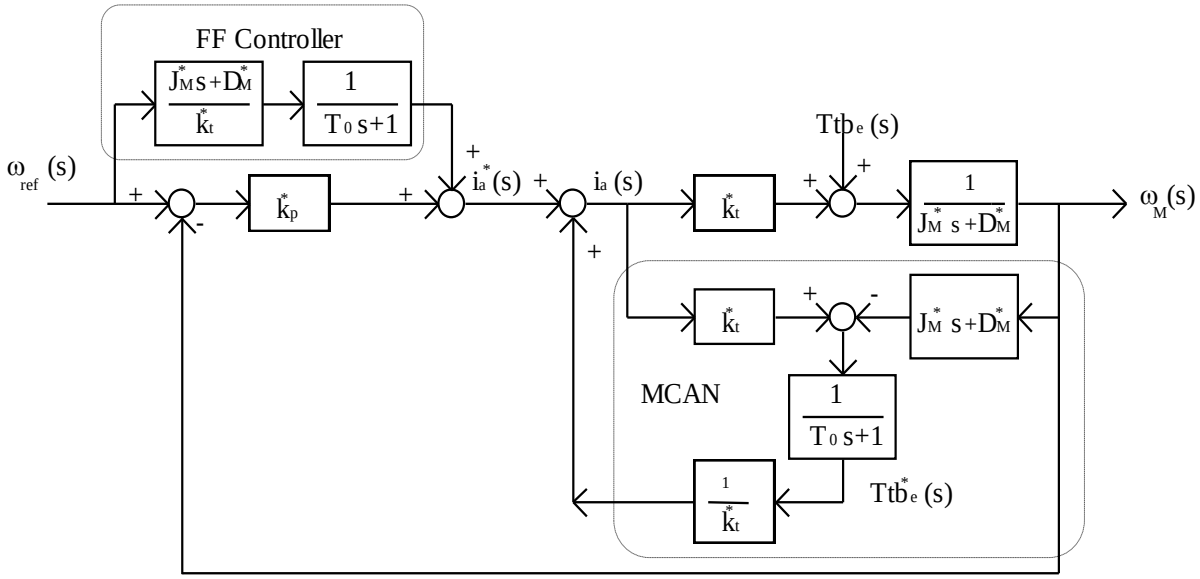

Figure 8. Block diagram of motor drive included equivalent disturbance observer and feed-forward controller

2. Flexible Cancelation (FCAN) Design

This observer design is constructed using the same method as the previous idea (in the MCAN design), which is based on the disturbance equivalent observer. Substituting the nominal and deviation values of the parameters, as determined before, into equation (19), the equivalent value of $T_{Le}(s)$ of $T_L(s)$ can be obtained and written as

$$T_{Le}(s) = \left(\frac{\Delta K_C}{s} + \Delta D_V\right)\Delta\omega(s) - (\Delta J_L s + \Delta D_L)\omega_L(s) - T_L(s) \tag{26}$$

or in the form of equivalent system, it can be written as,

$$T_{Le}(s) = (J_L^* s + D_L^*)\omega_L(s) - \left(\frac{K_C^*}{s} + D_V^*\right)\Delta\omega(s) \tag{27}$$

To get the estimated value of $T_{Le}^*(s)$ of $T_{Le}(s)$, the same idea as before, using a low pass filter is employed. Thus the equation below can be obtained.

$$T_{Le}^* = \frac{J_L^* s + D_L^*\omega_L(s) - \left(\frac{K_C^*}{s} + D_V^*\right)\Delta\omega(s)}{T_0 s+1} \tag{28}$$

After the signal $T_{Le}^*(s)$ is obtained, the aim is to inject this signal to the place where the equivalent disturbance T_{Le} is acting, or to the input, $\Delta\omega$ (see Figure 3). Thus, the signal disturbance will be canceled, as discussed before. However to do this is impossible, because in the physical system, this point is a torsion bar mechanism. So, the one thing that can be done is bring the signal and inject it into the input of the motor drive $i_a(s)$. Consequently, before the signal is injected at that point, it must be passed through the inverse of the motor drive transfer function, so that the dimension of the signal can be matched.

Finally, the block diagram of the complete FCAN can be as shown in Figure 9, where $\Delta\omega^*$ is the estimate of $\Delta\omega$.

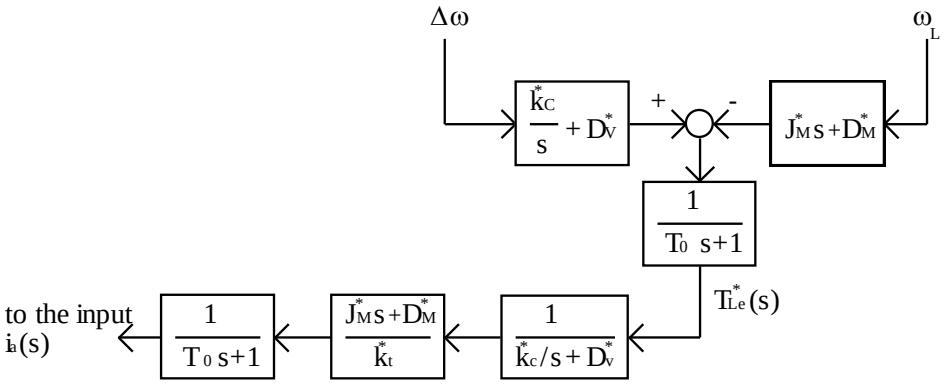

Figure 9. Block diagram of FCAN.

After the controllers are designed as discussed above, the complete system is build as well as the MCAN, FCAN and feed-forward controller as shown in Figure 10. In this block diagram the signal $\Delta\omega^*$ is connected to the input of the inversion motor drive and also to the input of MCAN, so as to eliminate the coupling effect between the motor drive and the load, or some times it is called *decoupling*.

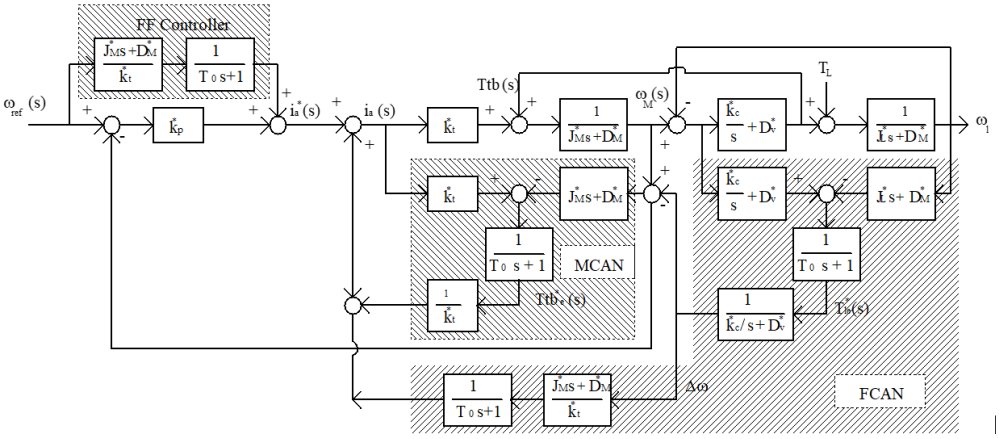

Figure 10. Block diagram of the Complete system using MCAN, FCAN and feed-forward controller.

Simulation Results

This control design have been simulation and the plant parameters used are J_M:0.07; J_L:0.17; D_M:0.005; D_L:0.01; D_V:0.5; k_C:500 and k_t:1. These parameters are from the real system that was adopted from factory. The value of observer parameters chosen by experiments are J^*_M: 0.07; J^*_L:0.17; D^*_M:0.005; D^*_L:10.00; D^*_V:2; k^*_C:500; k^*_t:1. The filters time constant are using T_0:0.0256; T_1:0.005; T_2:0.0256. For the ω_M, $\Delta\omega$ and ω_L filters used the same values, it is 0.0128. The simulation result are shown in Figure 11 and Figure 12. When 100% load is acting on the system the controller influences the speed motor drive, so that ω_M makes effort to keep the

output ω_L constant. This can be seen from the different signals of ω_L and ω_M as described in Figure 12. This happens because $\Delta\omega$ is injected into the feedback loop. Consequently, when $J_M > J_L$ then the frequency of the mechanical vibration is high, and the overall system becomes unstable and the proposed controller in this case is not satisfactory enough.

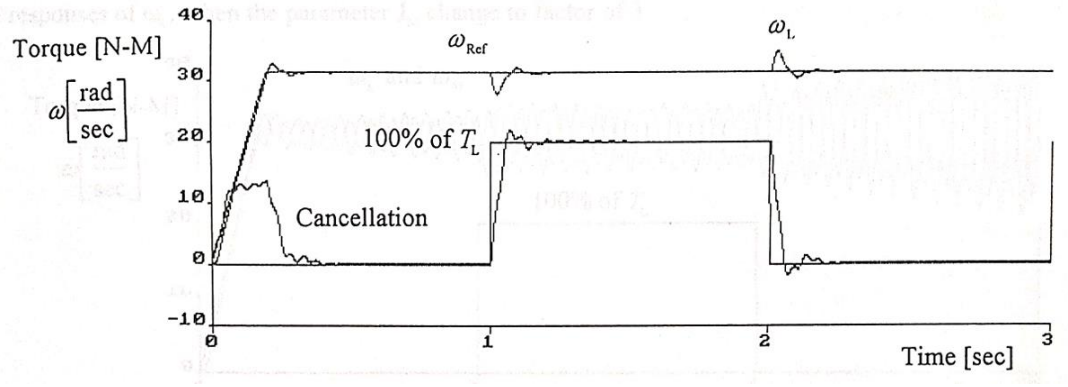

Figure 11. Respons time of speed load ω_L and cancelation signal when 100% disturbance.

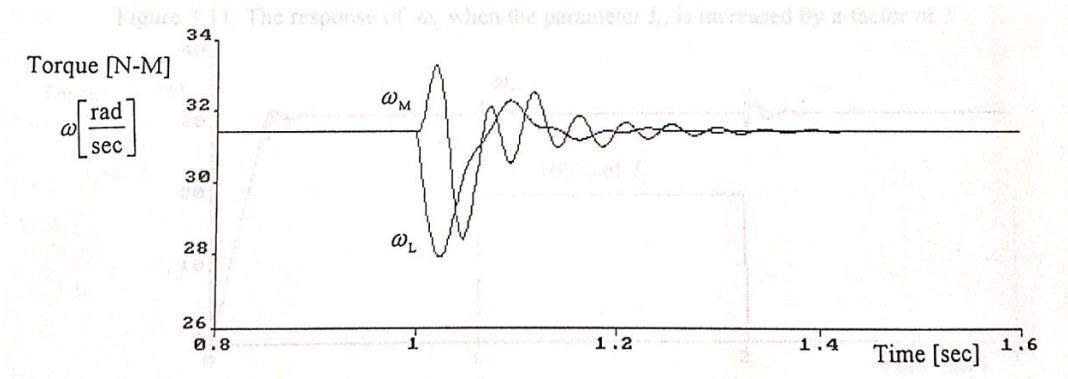

Figure 12. This graph illustrates how the motor dampens load vibrations.

Conclusion

The designed control method is composed of two parts. One is called MCAN, which is designed based on the motor site only (it does not compensate for the existing shaft and the load). The other 0ne is FCAN which compensates for the flexible shaft and load parts. When the motor inertia or load inertia is changed the overall system is possible to become unstable. This is because is injected into MCAN and if its frequency is too high; it is higher than that of the cutoff frequency of the controller, so that the controller cannot reduce it. To realize this control design, a processor with a speed fast enough to calculate all its Laplace mathematics is required.

References

[1] D.Devasena1, B.Sharmila2, Coimbatore S.Kaushik3, B,Priyadharshini4,"Advanced Controllers Implementation for Speed Control Analysis of Two Mass Drive System", Turkish Journal of Computer and Mathematics Education Vol.12 No.6(2021), 01-06

[2] A. Suyitno, Y. Dote, H. Kobayashi and J. Fujikawa, "Robust Vibration Control For Induction Motor Drive System Using Approximate Zeroing and Predictive Controller," Proceedings of the 5th Annual Conference of Industry Applications Society, IEE JAPAN-IAS'91 International Session, August 27-29. 1991 Sapporo, Japan, pp. E.33- E38.

[3] Ghazanfar Shahgholian, Pegah Shafaghi, Mansoor Zinali, Sepehr Moalem, ”State Space Analysis and Control Design of Two-Mass Resonant System”, 2009 Second International Conference on Computer and Electrical Engineering

[4]. Masanori Yukitomo, Takashi Shigemasa, Yasushi Baba, Fumio Kojima, “A Two Degrees of Freedom PID Control System, its Features and Applications”, 2004 5th Asia Control Conference, pp. 456 – 459.

[5] Ghazanfar Shahgholian, Member, IACSIT, ”Modeling and Simulation of a Two-Mass Resonant System with Speed Controller”, International Journal of Information and Electronics Engineering, Vol. 3, No. 5, September 2013

[8]. Takashi Shigemasa, Yasunori Negishi and Yasushi Baba, “A TDOF PID CONTROL SYSTEM DESIGN BY REFERRING TO THE MD-PID CONTROL SYSTEM AND ITS SENSITIVITIES”, 2013 European Control Conference (ECC) July 17-19, 2013, Zürich,Switzerland. pp. 3937 – 3942

[9]. Takashi Shigemasa, Yasunori Negishi and Yasushi Baba, “A TDOF PID CONTROL SYSTEM DESIGN BY REFERRING TO THE MD-PID CONTROL SYSTEM AND ITS SENSITIVITIES”, 2013 European Control Conference (ECC) July 17-19, 2013, Zürich, Switzerland. pp. 3937 – 3942

[10] Wen-Hua Chen, Jun Yang, Member, Lei Guo, and Shihua Li, Senior Member, ”Disturbance-Observer-Based Control and Related Methods—An Overview”, IEEE TRANSACTIONS ON INDUSTRIALELECTRONICS, VOL. 63, NO. 2, FEBRUARY2016

[11] Hideaki Hirahara, Kenshiro Kuroki, Shu Yamamoto, ”Simple Design Method of Two-Degree-of-Freedom PID Position Controller Based on Pole-Zero-Assignment for Linear Servo Motors”, 2020 23rd International Conference on Electrical Machines and Systems (ICEMS)

[12]. Lixiang Zhang, “Two Degree of Freedom Model Driven PID Control for Unstable Process with Times Delays”, Applied Mechanics and Materials Vol. 339 (2013) pp. 45- 49 @ (2013) Trans Tech Publocations, Switzerland.

[13]. Hideaki Hirahara; Kenshiro Kuroki; Shu Yamamoto,” Simple Design Method of Two-Degree-of-Freedom PID Position Controller Based on Pole-Zero-Assignment for Linear Servo Motors”, 2020 23rd International Conference on Electrical Machines and Systems (ICEMS)

[14]. Neha Jain; Mr. Hemant Kumar Vijayvergia, “Design & Analysis of 2-Dof PID Controller for Speed Control of DC Motor”, International Journal of Scientific & Engineering Research Volume 10, Issue 1, January-2019 ISSN 2229-5518

[15] Liyi Li; Genji Pei; Jiaxi Liu; Pengcheng Du; Le Pei; Chengbao Zhong, “2-DOF Robust H∞ Control for Permanent Magnet Synchronous Motor With Disturbance Observer”, IEEE Transactions on Power Electronics (Volume: 36, Issue: 3, March 2021)